

# Synthesis Parameter Influence on the Properties of Boron Doped Aluminum Nitride Thin Film Prepared by Co-sputtering

Zeng Yin Ong, Subramani Shanmugan, Devarajan Mutharasu

**Abstract**— Boron doped AlN (B,Al)N thin film on Si substrate was synthesized by co-sputtering using Al and B target at various gas mixture ratio (Ar : N<sub>2</sub>) and substrate temperatures. The prepared thin film was polycrystalline nature. The structural properties of prepared thin film was verified by XRD and the formation hexagonal AlN with (100) and (110) phases are confirmed. BN phases with different orientation was also noticed with the synthesized samples prepared at gas mixture ratio of Ar (6): N<sub>2</sub> (14) and Ar (8): N<sub>2</sub> (12). The intensity of the preferred peak increases as the N<sub>2</sub> gas ratio increases in the reaction gas mixture. The crystallinity was improved for the film prepared at 100°C substrate temperature using Ar (7): N<sub>2</sub> (13) gas mixture ratio. The surface morphology was evaluated using SEM and AFM and observed dense surface for the film prepared at 100°C substrate temperature. The film prepared at gas mixture ratio of Ar (8): N<sub>2</sub> (12) showed high surface roughness and particle size too. Overall, the gas mixture ratio and the substrate temperatures were influenced the growth of B doped AlN thin film on both structural and surface properties considerably.

**Index Terms** AlN, doping, thin film, co-sputtering, gas ratio, structural properties, surface properties.

## 1 INTRODUCTION

Group III nitrides gain their great significance in electronic and optoelectronic applications due to their advantages in wide band gap, thermal conductivity, thermal stability, and mechanical strength [1]-[2]. Among all the group III nitrides, Aluminum Nitride (AlN) has become the focus of material research because of its unique properties such as high thermal conductivity (260W m<sup>-1</sup>K<sup>-1</sup>), low thermal expansion coefficient, piezoelectric, high dielectric strength [3-5]. In addition, AlN has a thermal expansion which matches with silicon substrate. Besides that, AlN has been a critical buffer layer for the growth of GaN [6]-[7].

Special attention was paid to improve the properties of AlN through variation of process techniques and conditions such as distance between substrate with target, input power, deposition temperature, pressure, and gas ratio. W.J. Liu et al. [8] had reported on the influence of variations in synthesis parameters on the properties of deposited AlN film such as orientation textures and phase structure. Recent researchers have observed the improvement through doping of transition metal such as Sn [9] and Cr [10]. There were also few reports of B as doping material for AlN films [11]-[12]. Various techniques have been suggested and used to synthesize AlN film such as chemical vapour deposition (CVD) [13], reactive sputtering [14], pulsed laser deposition [15], and reactive molecular beam deposition [16]. Among these, reactive sputtering has the ad-

vantages over high temperature techniques such as low substrate temperature, good process control, high homogeneity along large substrate surface and good adhesion of the film the substrate. [17]-[18]. Co-sputtering is the method configured by two different target materials which can be sputtered with independent control over each target power. It was reported that such method can achieve attractive thin film properties, with also the possibility to synthesis multilayers, alloys, and graded compositions [19].

In this work, B-AlN thin films were synthesized on Si substrates by co-sputtering method for various synthesis parameters such as different gas mixture ratio (Ar and N<sub>2</sub> gas mixture ratio) and substrate temperatures. The structural analysis of sputtered samples was performed by using XRD technique and their structural parameters such as crystallite size, dislocation density, residual stress and strain etc were evaluated. The surface morphology of doped AlN thin film was investigated by FESEM and AFM respectively. The observed results are analyzed and discussed in this paper.

## 2 EXPERIMENTAL TECHNIQUE

### 2.1 (B,Al)N Thin Film Synthesis

The (B,Al)N thin films were deposited on Si (100) substrates by co-sputtering method using DC and RF power sources. Silicon substrates were selected in this study based on the thermal expansion coefficient of metal nitrides matches well with that of silicon [20]. The Si substrates were initially cleaned (RCA method) in a solution of H<sub>2</sub>O/HCl/H<sub>2</sub>O<sub>2</sub> (6:1:1 by volume) at 75 °C and a solution of H<sub>2</sub>O/H<sub>2</sub>O<sub>2</sub>/NH<sub>4</sub>OH (5:1:1 by volume) at 70 °C and then dipped into a dilute solution of 5 % HF to remove the surface oxides if any. After RCA cleaning, the substrates were rinsed in deionized water and blow-dried in N<sub>2</sub>.

- Zeng Yin Ong is currently pursuing his Master Degree in Applied Physics at School of Physics, University Science of Malaysia, Malaysia, PH:+60-012-4275601. E-mail: ongzenyin@gmail.com
- Subramani Shanmugan is currently working as a senior lecturer in School of Physics, University Science of Malaysia, Malaysia, PH:+60-04-6533672. E-mail: shagan77in@yahoo.co.in
- Devarajan Mutharasu is currently working as an Assoc. Professor in Nano Optoelectronics Research Laboratory, School of Physics, University Science of Malaysia, Malaysia, PH:+60-6533041. E-mail: mutharasu\_2000@yahoo.com

**TABLE 1**  
**DEPOSITION PARAMETERS MAINTAINED FOR (B, Al)N THIN FILM COATING BY CO-SPUTTERING**

Process	Gas Mixture Ratio	Substrate Temp.
Process 1	Ar (6) : N <sub>2</sub> (14)	R.T.
Process 2	Ar (7) : N <sub>2</sub> (13)	R.T.
Process 3	Ar (8) : N <sub>2</sub> (12)	R.T.
Process 4	Ar (7) : N <sub>2</sub> (13)	100 °C
Process 5	Ar (7) : N <sub>2</sub> (13)	200 °C

The sputtering process was conducted by using pure Al (99.99 % purity) target (3 inch in diameter and 4 mm in thickness) and B (99.99 % purity) target (3 inch in diameter and 4 mm in thickness). Al was deposited by DC sputtering and Boron was deposited by RF sputtering since it is poor electrical conductor [21]. The chamber was loaded with cleaned substrates fixed on substrate holder and initially pump down into high vacuum state (10<sup>-5</sup> mbar) by using a turbo molecular pump backed by a rotary pump. High pure Ar (99.999%) and N<sub>2</sub> (99.999%) were both functioned as sputtering gas and reactive gas respectively. Prior to film deposition process, pre-sputtering was carried out for about 5 -10 minutes in order to remove the surface oxidation of the targets. To get the uniform thickness, rotary drive system was used at a rate of 25 RPM throughout all the process with distance between substrates to target of 7 cm. All coatings were conducted under the discharge power at 100 W DC power (Al) and 50 W RF power (B). The chamber pressure was maintained at (8.00-9.00) × 10<sup>-3</sup> mbar and the coating process time was carried out for about one hour. The thin films were deposited for five different synthesis parameters by changing the Ar and N<sub>2</sub> gas mixture ratio and substrate temperature. The parameters used for this study is as shown in Table 1. The X-ray diffraction analysis (XRD) was carried out using X-ray diffractometer (XRD, X'pert-PRO, Philips, Netherlands). The surface morphology was examined using field emission scanning electron microscope (FESEM, Nova Nano-SEM 450) and atomic force microscope (AFM, Dimension Edge, Bruker).

### 3 RESULTS AND DISCUSSION

#### 2.2 Final Stage

The xrd spectra of all films are recorded as shown in Figure 1 (a) and (b). The spectra shows that the formation of hexagonal phase of AlN in all samples. It is also observed that intense peak was noticed with h(100) oriented phase for all samples. Additionally, h(110) oriented phase is also existing in the sample samples with noticeable change in intensity. From the Figure 1(a), it clearly indicates the influence of reactive gas (N<sub>2</sub>) flow on the crystalline nature as well as the compound formation. Fig 1a indicates the formation of cubic and orthorhombic BN phases only with process 1 and process 3. Surprisingly, no peak could be observed with process 2 conditions. It shows that the film prepared at process 2 conditions i.e., Ar (7): N<sub>2</sub> (13) has amorphous structure than other two gas mixture ratio.

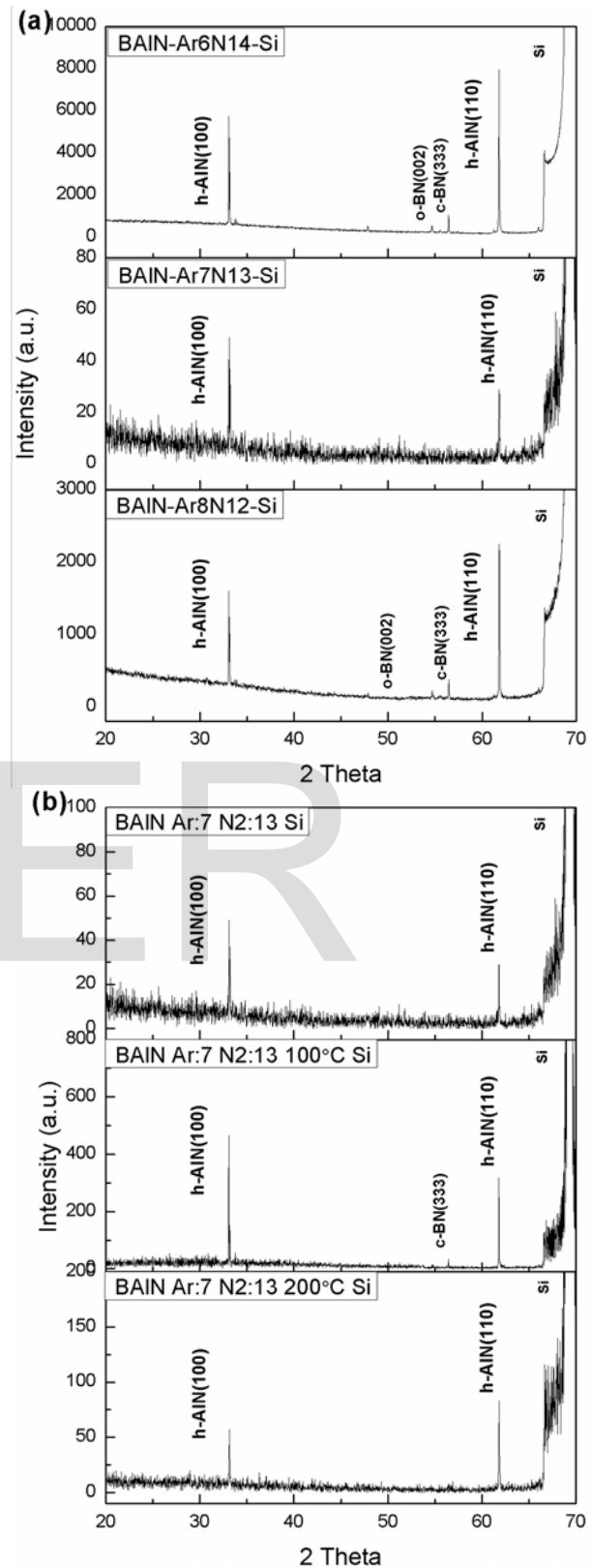


Fig. 1(a) and (b). XRD spectra of co-sputtered (B, Al)N thin film at various process conditions. (a) XRD spectra for various gas ratio and (b) XRD spectra of (B, Al)N thin film prepared at Ar(7):N<sub>2</sub>(13) with substrate temperatures (100 and 200°C)

On considering the gas mixture ratio particularly in process 1 and process 3, the crystalline quality of the (B, Al)N thin film is high than that of the film prepared by process 2. A drastic reduction on crystalline quality could be noticed with gas ratio of Ar (7): N<sub>2</sub> (13). Though, the intensity of xrd peaks are high for process 1 and process 3 samples, a noticeable decrease in peak intensity is observed for the samples prepared at Ar (8): N<sub>2</sub> (12) gas mixture ratio. Additionally, cubic and orthorhombic phases are noticed with process 1 and process 3. In order to see the effect of growth temperature, the gas mixture ratio was fixed and the two different substrate temperatures were used to grow the (B, Al)N thin film and the xrd spectra were recorded as shown in Figure1(b).

It clearly shows that the intensity of (100) and (110) oriented peaks increases for 100 °C substrate temperatures and decreases on higher substrate temperature (200 °C). Generally, the temperatures improve the crystallite quality and hence we observe the increased intensity. In our study, at high substrate temperatures, the intensity decreases noticeably for both (110) and (100) orientations. It may be due to the alignment of B atoms in the AlN lattice at high temperatures. To understand clearly, the structural properties of the prepared (B,Al)N thin film was measured from the XRD spectra and summarized in Table 2. According to Table 2, c-BN peak related to (333) orientation can be found in process 1, 3 and 4 i.e., with gas ratio of Ar (6): N<sub>2</sub> (14) (RT), Ar 8 : N<sub>2</sub> 12 (RT), and Ar (6): N<sub>2</sub> (14) (100 °C).

The xrd spectra of the samples prepared at gas ratio of Ar (7): N<sub>2</sub> (13) (R.T) and Ar (7): N<sub>2</sub> (13) (200 °C) show no peak of BN which is due to the B atoms diffused into the AlN crystal structures. It is assumed that the B atom diffuses at high temperatures during the synthesis and evidence of doping. It is validated by observing the peak shift from lower 2θ angle to higher 2θ angle [22]. This observation could be noticed with h(100) and h(110) from our XRD results. From the xrd results, the lattice constant shrinkage was noticed with h(110) phase and low value was observed for the film prepared by process

2, process 4 and process 5 (2.121 Å). A high value is observed with process 1 (2.947 Å) followed by process 3 (2.366 Å). This may possibly due to incorporation of B dopants lead to decrease of a-plane lattice constant, this indicates that B dopant occupying the substitutional lattice sites of the h-AlN(110) crystal structure [23].

To understand the structural changes and properties, the structural parameters are evaluated from the xrd results and the The crystallite size is calculated by using Debye Scherer formula [24]:

$$D = 0.94\lambda/\beta\cos\theta \quad (1)$$

where λ is wavelength (in Angstrom), β is the broadening of diffraction peak (in radians), θ is the Bragg diffraction angle.

The measured crystallite size are summarized in table 2 and noticed that the gas mixture ratio influence the crystallite size noticeably especially for hexagonal phases. From the Table 2, the crystallite size increases as the N<sub>2</sub> gas ratio decreases. Considerable crystallite size reduction could be observed for the process 4 and 5 at fixed gas ratio of Ar (7) : N<sub>2</sub> (13).

The internal stress (σ) in the deposited film is calculated using the relation:

$$\sigma = -E(d_a - d_o)/(2d_oY) \quad (2)$$

Where d<sub>o</sub> and d<sub>a</sub> are the d spacing of bulk and thin film forms respectively [25]. E and Y are Young's modulus and Poisson's ratio of AlN are E = 308 GPa [26], Y = 0.29 [27], and BN E = 748 GPa [28], Y = 0.19 [29] respectively. The internal stress developed during the growth of (B, Al) N thin film was calculated for all samples and the observed results are given in Table 3. As seen in Table 3, the stresses are decreasing as with N<sub>2</sub> gas ratio increasing. The highest value in stress is observed for the samples prepared by process 4 (at substrate temperature of 100°C). It is also observed from the Table 3 that the compressive stress could be observed with h(110) phases for all processing conditions.

In addition to this, dislocation density (δ), defined as the length of dislocation lines per unit volume of crystal, was evaluated from relation [30]:

TABLE 2  
STRUCTURAL PROPERTIES OF (B, AL)N THIN FILM PREPARED WITH DIFFERENT GAS RATIO

Process	Identity	Observed 2θ (°)	Standard 2θ (°)	FWHM (°)	Crystallite size (nm)	Lattice parameter (Å)
Process 1	h-AlN (100)	33.075	33.095	0.048	172.59	2.379
	o-BN (002)	54.674	54.759	0.096	93.127	3.354
	c-BN (333)	56.452	56.860	0.072	125.19	10.826
	h-AlN (110)	61.801	59.350	0.096	96.411	2.947
Process 2	h-AlN (100)	33.203	33.095	0.059	140.37	2.696
	h-AlN (110)	61.816	59.350	0.079	117.58	2.121
Process 3	h-AlN (100)	33.067	33.095	0.059	140.32	2.546
	o-BN (002)	54.704	54.759	0.079	113.59	3.354
	c-BN (333)	56.479	56.860	0.079	114.52	11.803
	h-AlN (110)	61.829	59.350	0.072	128.57	2.366
Process 4	h-AlN (100)	33.074	33.095	0.059	140.32	2.706
	c-BN (333)	56.462	56.860	0.048	187.79	8.464
	h-AlN (110)	61.818	59.350	0.072	128.46	2.121
Process 5	h-AlN (100)	33.133	33.095	0.059	140.34	2.702
	h-AlN (110)	61.833	59.350	0.098	94.080	2.121

**TABLE 3**  
INTERNAL STRESS, DISLOCATION DENSITY AND STRAIN OF CO-SPUTTERED (B, AL)N THIN FILM

Process	Identity	Internal Stress (MPa)	Dislocation density (m <sup>-2</sup> )	Strain
Process 1	h-AlN (100)	0.3093	3.36×10 <sup>13</sup>	0.000705
	o-BN (002)	2.3475	1.15×10 <sup>14</sup>	0.000810
	c-BN (333)	12.931	6.28×10 <sup>13</sup>	0.000585
	h-AlN (110)	-20.019	1.08×10 <sup>14</sup>	0.000699
Process 2	h-AlN (100)	0.5393	5.08×10 <sup>13</sup>	0.000863
	h-AlN (110)	-20.137	7.23×10 <sup>13</sup>	0.000573
Process 3	h-AlN (100)	0.4281	5.08×10 <sup>13</sup>	0.000867
	o-BN (002)	2.3475	7.75×10 <sup>13</sup>	0.000664
	c-BN (333)	12.054	7.63×10 <sup>13</sup>	0.000639
	h-AlN (110)	-20.245	6.05×10 <sup>13</sup>	0.000524
Process 4	h-AlN (100)	2.553	5.08×10 <sup>13</sup>	0.000867
	c-BN (333)	12.619	2.84×10 <sup>13</sup>	0.000390
	h-AlN (110)	-20.160	6.05×10 <sup>13</sup>	0.000524
Process 5	h-AlN (100)	1.6287	5.07×10 <sup>13</sup>	0.000268
	h-AlN (110)	-20.278	1.12×10 <sup>14</sup>	0.000500

$$\delta = 1/D^2 \quad (3)$$

The dislocation density is mainly based on the crystallite size and hence it differs as a result of change in crystallite size. It is the measure of structural defects. Since the dislocation density is measured based on the crystallite size, the observed results are obeyed the behaviour of changing the crystallite size for different process conditions.

The strain ( $\epsilon$ ) is calculated from formula using XRD results:

$$\epsilon = \beta \cot \theta / 4 \quad (4)$$

The calculated values are summarized in Table 3 and show that the strain value increases for h(100) phase and decreases for h(110) phases as with N<sub>2</sub> gas ratio increases. The strain during the synthesis of thin film at substrate temperature showed reduced value than prepared at room temperature.

### 3.2 Surface Analysis

To verify the thickness of all prepared samples, the cross sectional images of all samples were recorded by FESEM and observed the average thickness of each samples as given in Table 4. It clearly shows that the higher thickness is achieved with process 3 conditions which may be attributed to the higher Ar percentage during sputtering process. From Table 4, it is also observed that the thickness decreases as the substrate temperature increases for the samples prepared using process 2. Additionally, the surface morphology of the film prepared using various process conditions is recorded and presented as shown in Figure 2.

The film synthesized with Ar (6): N<sub>2</sub> (14) gas mixture ratio shows uniform surface morphology and also dense surface with nano size particles. But the surface damage such as pores and flaw could be observed for the film prepared at high low N<sub>2</sub> concentration ie for high Ar ratio in the gas mixture. The surface damages was rectified by preparing the film at 100 °C

**TABLE 4**  
AVERAGE THICKNESS OF CO-SPUTTERED (B, AL)N THIN FILM FOR DIFFERENT SPUTTERING PROCESS

Process	Average Thickness (nm)
Process 1	201.1
Process 2	180.7
Process 3	303.1
Process 4	126.8
Process 5	99.8

**TABLE 5**  
VARIATION OF SURFACE ROUGHNESS AND PARTICLE SIZE AT DIFFERENT SPUTTERING GAS RATIOS

Process	Roughness, Ra (nm)	Particle Size, Ra (nm)
Process 1	1.37	369.26
Process 2	1.06	288.16
Process 3	11.1	609.86
Process 4	1.57	260.77
Process 5	1.01	310.50

for process 2 samples and good surface morphology was noticed with the samples prepared at substrate temperature. In addition, particle agglomeration is also noticed for the samples prepared at 200 °C with the gas mixture ratio of Ar (7): N<sub>2</sub> (13).

To understand the influence of process parameters on surface morphology, the surface topography of all samples were captured by AFM and the images were processed for analysis. The processed images are given in Figure 3. It reveals that a distinct surface changes are noticed with the N<sub>2</sub> gas ratio increases. Surface damage could be noticed and the density increases considerably. To study in detail, all images are processed using nanoscope software and the surface roughness and the particle size are measured as given in Table 5.

It clearly depicts that the roughness increases with N<sub>2</sub> concentration increases in the processing gas mixture. The samples prepared using process 3 shows high surface roughness of 11 nm. It is also noticed that low value in roughness is possible with process 2 and process 5 where we observed no other peaks than hexagonal phase. At 100 °C substrate temperature, the roughness value increases for the film processed at Ar (7) : N<sub>2</sub> (13) gas mixture ratio. A noticeable reduction in surface roughness could be observed with substrate temperature of 200 °C for the process 5 gas mixture ratio. On considering particle size, the film prepared at process 3 conditions shows higher particle size than all other samples. The linear changes could be observed between the surface roughness and the particle size i.e., the surface roughness increases as with particle size increases. When compared to thickness of each film, the similarity could be seen for the surface parameters and hence higher thickness films show high surface roughness and also bigger particles.

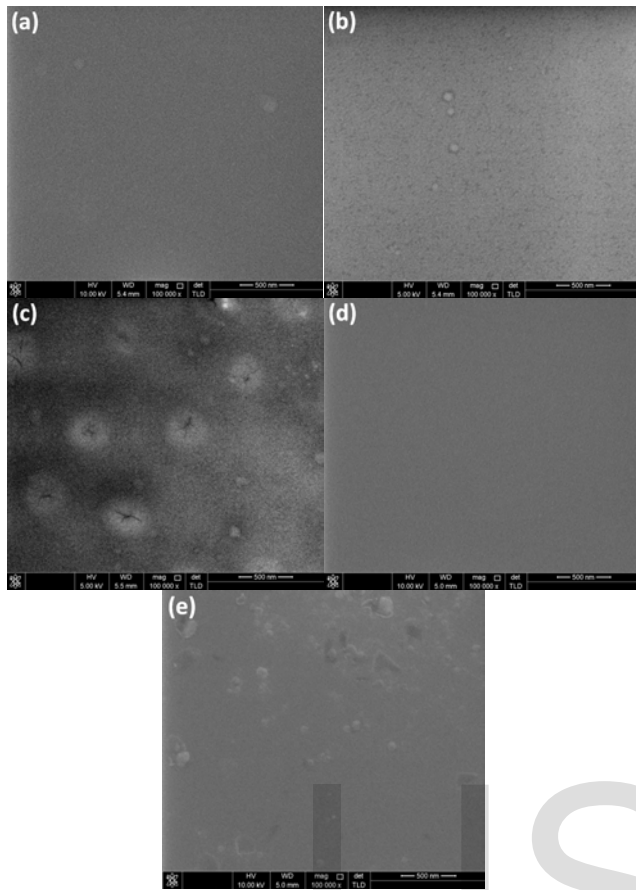


Fig. 2. FESEM images of co-sputtered (B, Al)N thin film surface prepared using (a) Process 1, (b) Process 2, (c) Process 3, (d) Process 4 and (e) Process 5 conditions.

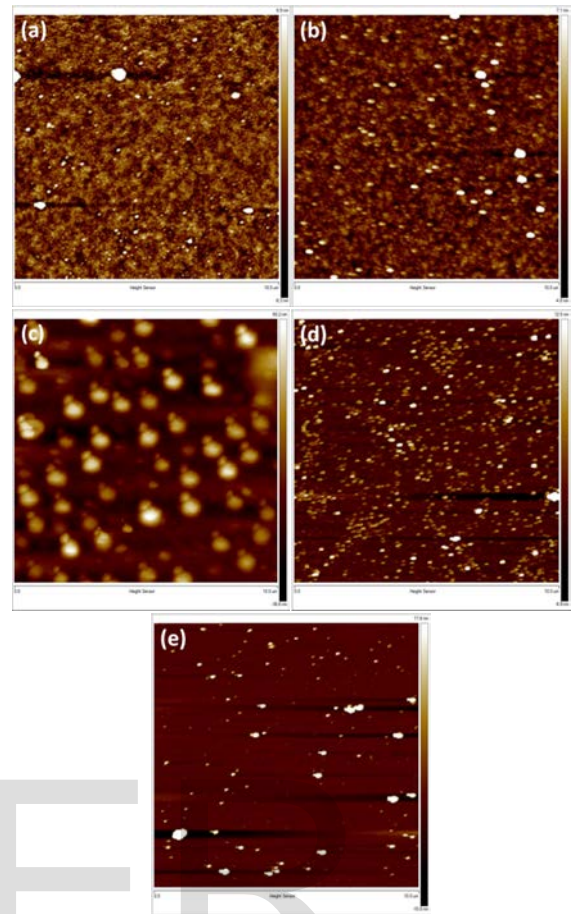


Fig. 3. The surface topography of AFM images of (B, Al)N thin film surface of (a) Process 1, (b) Process 2, (c) Process 3, (d) Process 4, (e) Process 5.

## 4 CONCLUSION

Co-sputtering was used to prepare B doped AlN thin film on Si substrates at different gas mixture ratio and substrate temperatures. Hexagonal phase with (100) and (110) orientations was evidenced the formation of polycrystalline structure of synthesized B doped AlN thin film. The crystalline nature was affected by gas mixture ratio as well as substrate temperature and improved crystallinity was noticed with gas mixture with high N<sub>2</sub> content. The other structural properties such as crystallite size, strain, stress and dislocation density were also affected by the synthesis parameters. The formation of BN phase also influenced the crystal growth of AlN thin film. The surface roughness and the particle size were high for the film prepared at low N<sub>2</sub> content in the gas mixture ratio.

## ACKNOWLEDGMENT

This work was financially supported by Collaborative Research in Engineering, Science and Technology (CREST) under grant (304/PFIZIK/650601/C121). The author would also like to thank the lab staff M. Abu Bakar from X-Ray Crystallography Lab who is supporting in this work. It is acknowledged for the facilities provided by NOR lab at school of physics for

B doped AlN thin film synthesis and characterization.

## REFERENCES

- [1] Z. C. Feng, "III-Nitride Semiconductor Materials," National Taiwan University, March 2006.
- [2] O Ambacher, "Growth and applications of Group III-nitrides," *J. Phys. D: Appl. Phys.*, vol. 31, pp. 2653, 1998.
- [3] J. Chaudhuri, L. Nyakiti, R.G. Lee, Z. Gu, J.H. Edgar, and J.G. Wen, "Thermal oxidation of single crystalline aluminum nitride," *Materials Characterization*, vol. 58(8-9), pp. 672-679, Aug/Sep 2007.
- [4] J. Olivares, S. González-Castilla, M. Clement, A. Sanz-Hervás, L. Vergara, J. Sangrador, and E. Iborra, "Combined assessment of piezoelectric AlN films using X-ray diffraction, infrared absorption and atomic force microscopy," *Diamond and Related Materials*, vol. 16(4-7), pp. 1421-1424, Apr/Jul 2007.
- [5] A. Dollet, Y. Casaux, G. Chaix, and C. Duppy, "Chemical Vapour Deposition of Polycrystalline AlN Films from AlCl<sub>3</sub>-NH<sub>3</sub> Mixtures. Analysis And Modelling of Transport Phenomena," *Journal of Thin Films*, vol.406, pp. 1-6, 2002.
- [6] S. Nakamura, "In Situ Monitoring of GaN Growth Using Interference Effects," *Jpn. J. Appl. Phys.*, vol. 30 pp. 1620, 1991.
- [7] I. Akasaki, H. Amano, Y. Koide, K. Hiramatsu, and N. Sawaki, "Effects of ain buffer layer on crystallographic structure and on electrical and optical properties of GaN and Ga<sub>1-x</sub>Al<sub>x</sub>N (0 < x ≤ 0.4) films

- grown on sapphire substrate by MOVPE," *Journal of Crystal Growth*, vol. 98(1-2), pp. 209-219, November 1989.
- [8] W.J. Liu, S.J. Wu, C.M. Chen, Y.C. Lai, and C.H. Chuang, "Microstructural evolution and formation of highly c-axis-oriented aluminum nitride films by reactively magnetron sputtering deposition," *Journal of Crystal Growth*, vol. 276(3-4), pp. 525-533, Apr 2005.
- [9] M. Moreira, J. Bjurström, I. Katardjev, and V. Yantchev, "Aluminum scandium nitride thin-film bulk acoustic resonators for wide band applications," *Vacuum*, vol. 86(1), pp. 23-26, Jul 2011.
- [10] V.V. Felmetzger, and M.K. Mikhov., "Reactive magnetron sputtering of piezoelectric Cr-doped AlN thin films," *Ultrasonics Symposium (IUS), 2011 IEEE International*, vol., no., pp. 835,839, Oct. 2011.
- [11] L. Liljeholm, M. Junaïd, T. Kubart, J. Birch, L. Hultman, I. Katardjiev, "Synthesis and characterization of (0001)-textured wurtzite Al<sub>1-x</sub>B<sub>x</sub>N thin films," *Surface and Coatings Technology*, vol. 206(6), pp. 1033-1036, Dec 2011.
- [12] M. Witthaut, R. Cremer, and D. Neuschütz, "Electron spectroscopy of single-phase (Al,B)N films," *Surface and Interface Analysis*, vol. 30(1), pp 580-584, Sep 2000.
- [13] K.M. Lakin, "Thin film resonators and filters," *Ultrasonics Symposium, 1999. Proceedings. 1999 IEEE*, vol. 2, no., pp. 895-906, 1999.
- [14] I. Ivanov, L. Hultman, K. Järrendahl, P. Mårtensson, J.E. Sundgren, B. Hjörvarsson, and J.E. Greene, "Growth of epitaxial AlN(0001) on Si(111) by reactive magnetron sputter deposition," *Journal of Applied Physics*, vol. 78, pp. 5721-5726, 1995.
- [15] R.D. Vispute, V Talyansky, R.P. Sharma, S Chooopun, M Downes, T Venkatesan, Y.X Li, L.G Salamanca-Riba, A.A Iliadis, K.A Jones, and J. McGarrity, "Advances in pulsed laser deposition of nitrides and their integration with oxides," *Applied Surface Science*, vol. 127-129, pp. 431-439, May 1998.
- [16] S. Yoshida, S. Misawa, Y. Fujii, S. Takada, H. Hayakawa, S. Gonda, and A. Itoh, "Reactive molecular beam epitaxy of aluminium nitride," *Journal of Vacuum Science & Technology*, vol.16, pp. 990-993 Jul 1979.
- [17] J.P. Huang, L.W. Wang, Q.W. Shen, C.L. Lin, and M. Östling, "Preparation of AlN thin films by nitridation of Al-coated Si substrate," *Thin Solid Films*, vol. 340(1-2), pp. 137-139, Feb 1999.
- [18] S.S Lin, and J.L. Huang, "Effect of thickness on the structural and optical properties of ZnO films by r.f. magnetron sputtering," *Surface and Coatings Technology*, vol. 185(2-3), pp. 222-227, Jul 2004.
- [19] S. K. Rawal, and R. Chandra, "Wettability and Optical Studies of Films Prepared from Power Variation of Co-sputtered Cr and Zr Targets by Sputtering," *Procedia Technology*, vol. 14, pp. 304-311, 2014.
- [20] X.H. Xu, H.S. Wu, C.J. Zhang, and Z.H. Jin, "Morphological properties of AlN piezoelectric thin films deposited by DC reactive magnetron sputtering," *Thin Solid Films*, vol. 388(1-2), pp. 62-67, Jun 2001.
- [21] P. J. Gielisse H. Niculescu Y. Xu N. Bai M. Tu, "Vapor Deposition Equipment and Thin Film Processing," Technical Report, Accession no. AD-A321 245/3, Florida A&M University, College of Engineering, Aug 1996.
- [22] J.H. Song, J.L. Huang, H.H. Lu, and J.C. Sung, "Investigation of wurtzite (B,Al)N films prepared on polycrystalline diamond," *Thin Solid Films*, vol. 516(2-4), pp. 223-227, Dec 2007.
- [23] A.Y. Polyakov, N.B. Smirnov, A.V. Govorkov, R.M. Frazier, J.Y. Liefer, G.T. Thaler, C.R. Abernathy, S.J. Pearton, and J.M. Zavada, "Properties of highly Cr-doped AlN," *Applied Physics Letters*, vol. 85, no.18, pp. 4067-4069, Nov 2004.
- [24] G. Gordillo, J.M. Flrez and L.C. Hernandez, "Preparation and characterization of CdTe thin films deposited by CSS," *Sol. Energy Mater. Sol. Cells*, vol. 37, pp. 273-281, 1995.
- [25] A.J. Perry, "The state of residual stress in TiN films made by physical vapor deposition methods; the state of the art." *Journal of Vacuum Science & Technology A: Vacuum, Surfaces, and Films*, vol. 8(3), pp. 1351-1358, 1990.
- [26] D. Gerlich, S.L. Dole, and G.A. Slack, "Elastic properties of aluminum nitride." *Journal of Physics and Chemistry of Solids*, vol. 47(5), pp. 437-441, 1986.
- [27] R. Thokala, and J. Chaudhuri, "Calculated elastic constants of wide band gap semiconductor thin films with a hexagonal crystal structure for stress problems," *Thin Solid Films*, vol. 266(2), pp. 189-191, 1995.
- [28] "Boron Nitride, Mechanical Properties, Elastic Constants, Lattice Vibrations," *New Semiconductor Materials Archive*. Retrieved August 13, 2014, <http://www.ioffe.ru/SVA/NSM/Semicond/BN/mechanic.html>
- [29] A.R. Stokes, and A.C.J. Wilson, "The diffraction of X rays by distorted crystal aggregates - I," *Proceedings of the Physical Society*, vol.56, pp. 174, 1944.
- [30] G.B. Williamson and R.E.Smallman, "Dislocation densities in some annealed and cold-worked metals from measurements on the X-ray debye-scherrer spectrum," *Philos. Mag.*, vol. 1, pp. 34-46, 1956.